*Proceedings of the Twenty-fifth (2015) International Ocean and Polar Engineering Conference* **www.isope.org**
*Kona, Big Island, Hawaii, USA, June 21-26, 2015*

*ISBN 978-1-880653-89-0; ISSN 1098-6189*

# Diffusion Model Identification for Long-Term Coastal Profile Evolution

*Mikhail M. Lavrentiev, Renato Spigler, Eldar Goryunov, Alexey A. Romanenko*

Department of Information Technologies, Novosibirsk State University Novosibirsk,

University "Roma Tre" Rome, Italy

Institute of Automation and Electrometry Novosibirsk, Russia

## ABSTRACT

As it was found relatively recently, behavior-oriented diffusion models reasonably describes the time evolution of the cross-shore position of coastal profiles. Two time-independent coefficients in the governing equation, which embody the relevant physical properties, are identified simultaneously. Earlier, the authors have validated and calibrated numerically the proposed model, processing two sets of real data, the first measured over 10 years at Duck, in North Carolina (USA), the second obtained over 39 years measurements at Delfland (Holland). Here, the model dependence on the alongshore position of the observation point is studied. The coefficients of the model equation are determined by means of a certain iteration process. As it was observed, the achieved convergence is now better than when several separate observations along the coast are involved.

KEY WORDS: Coastal profile; evolution; modeling; parameters identification.

## INTRODUCTION

It is well known that erosion and accretion phenomena are responsible for modifications of the coastal environment, and thus have been a source of growing concern among coastal engineers. Taking into account human activities, a special study is needed to predict the impact of coastal zone management. To introduce the reader to this subject, we refer to the ideas of Avdeev et al. (2009).

In Larson et al. (1987), a diffusion-type equation has been derived applying mass conservation to the *1*-line model of coastal profiles. The diffusion coefficient in the governing equation, having the physical dimension of a square length divided by time, corresponds to the time scale of shoreline change, following a disturbance (a wave action, e.g.). A high amplitude of the long-shore sand transport rate produces a rapid shoreline response, so that a new state of equilibrium with the incident waves is attained. Furthermore, a larger "depth of closure" indicates that a larger part of the beach profile participates in the sand movement, thus leading to a slower shoreline response. We recall that the depth of closure, i.e. the seaward limit of any significant net sediment transport, has been typically estimated by comparing beach profiles, determining where vertical changes become negligible. In Beavers et al. (1999), downward-looking sonar altimetries were used at Duck, North Carolina (USA), to survey the value of the depth of closure due to environmental conditions and time scales.

The aforementioned diffusion model, presented in De Vriend et al. (1993), is the following:

$$\frac{\partial(\delta X)}{\partial t} = D(z)\frac{\partial^2(\delta X)}{\partial z^2} + \phi\left(t, z, \delta X, \frac{\partial(\delta X)}{\partial z}\right) \qquad (1)$$

Here, $\delta X(t,z)$ represents the change of cross—shore position (namely, the change in the depth at the distance $z$ from the shoreline) of the coastal profile, and $D(z) > 0$ is the diffusion coefficient.

Following De Vriend et al. (1993), we give some explanations for a special case of the term $\phi\left(t, z, \delta X, \frac{\partial(\delta X)}{\partial z}\right)$. If $\phi = S(t,z)$ (which represents a source term), it is possible to introduce the effects of a random forcing, long-shore transport gradients, and human interference, such as nourishment and sand mining, cf. De Vriend et al. (1993).

The linear choice $\phi = B(z)\partial(\delta X)/\partial z$, or $\phi = B(z)\delta X$, is also interesting in view of applications. In these models, the coefficient $B(z)$ represents the velocity of long-shore sand waves movement. Thus, the collective movement of long-shore sand

waves can be described in addition to a particular movement. This means that the motion of sediments is characterized by two scales: a relatively rapid movement of sand particles, and a relatively slow collective movement of sand bodies. Clearly, all process-based and empirical knowledge is stored in the coefficients *D(z)* and *B(z)* as well as in the boundary conditions to be associated to Eq. 1. In this paper, we assume $\phi = B(z)\delta X + f(t)$ in Eq. 1. In over words, following De Vriend et al. (1993), we suppose that the long-term evolution of coastal lines, such as the cross-shore profile, is described by the diffusion equation

$$u_t = D(z)u_{zz} + B(z)u + f(t) \tag{2}$$

along with suitable Initial and Boundary Data. This model states that changes in the bathymetry (that is the elevation of the seafloor) rests on two space-dependent coefficients as well as on a time-dependent source-term, the wave height.

Here *u(z,t) = p(z,t) - p(z,0), p(z,t)* denoting the depth profile and thus *u(z,t)* represents changes of the cross-shore profile. Throughout the paper, the letter *p* will denote profiles, while *u* will represent the difference between current profiles and the initial profile. Concerning some general approaches to study the long-term coastal profile evolution, see Bakker (1968), Capobianco (1992), Dean (1991), Hanson (1987), Larson et al. (1987). The two functional coefficients, *D(z)* and *B(z),* which embody macroscopically all the relevant physical processes, are unknown, and it seems very hard to conceive any derivation of them from prime physical principles, or by means of purely physical measurements. The source term, *f(t),* is associated with wave conditions, in fact it represents the average wave height. As was already mentioned, a *validation* of the model proposed by De Vriend et al. (1993) was obtained in Avdeev et al. (2009). As it was already observed, models like that in Eq. 2 reasonably describes depth profile evolution, that is the cross shore at a certain single point of the coast. Note that data sets measured at two geographic locations (in the USA and in Holland) and with essentially different structure, were considered. Moreover, the possibility of 1-2 years prediction of the depth profile evolution was demonstrated.

In this work, by using modern computer facilities, we include into consideration the along-shore dependence of the depth profiles. We apply the same model, where the coefficients, *D* and *B,* only depend on the cross-shore distance, *z*, to describe the depth profile evolution on a certain interval along the shore line.

The rest of the paper is arranged as follows. First of all, the mathematical formulation of the problem is given, following Avdeev et al. (2009). Then, we describe the structure of the measured data and recall some of the results earlier obtained, in which only one observation point at the coast was used. Proceeding as in Avdeev et al. (2009), we run some numerical tests using 30 points along the coast. Finally, the problem is calibrated under the assumption that the coefficients *D* and *B* may take different values at each of 10 observation points along the coast. In all cases, *D* and *B* are assumed to be piecewise constant, taking 15 (different) values at equal cross shore interval.

## STATEMENT OF THE PROBLEM

A validation of the model proposed in De Vriend et al. (1993) was obtained proceeding along the following lines. Knowing *experimentally* the solution, say $u^{exp}(z, t)$, in the space-time domain $Q_T = \{(z,t) : 0 \le t \le T, 0 \le z \le H\}$, for some $H > 0$ and $T > 0$ (at the grid-points where the measurements were made, i.e. at Delfland), we can compute the Initial-Value (IV), $u^{exp}(z,0)$ (note that $u^{exp}(z,0) = 0$ in case we describe *changes* of the coastal profile), and the Boundary-Values (BVs), $u^{exp}(H,t)$, $\partial u^{\exp} \partial z(0,t)$. The latter quantity was obtained, in practice, computing a differential quotient, namely $\left(u^{\exp}(\Delta z, t) - u^{\exp}(0,t)\right)\Delta z$, for a space-step $\Delta z$ sufficiently small. While *T* could be any sufficiently long final observation time (in order to be able to infer the long-time behavior of the coastal line evolution), the parameter *H* can be thought of as an estimate of the so-called "distance of closure" (or depth of closure), that is the location where the simulated diffusive and transport phenomena virtually end, or, in other words, it represents the seaward limit of significant net sediment transport.

*Assuming* that the underlying model might be represented by the diffusion equation, Eq. 2, and starting from some "initial guess" for the coefficients *B(z)* and *D(z),* both taken piecewise constant with *z*, we use a suitable inversion algorithm (based on the minimization of a certain cost functional) to obtain iteratively a better approximation, also *piecewise constant* with *z*, say $B_n$ and $D_n$, at the *n*-th iteration, for the two coefficients, simultaneously.

While we do *not* know the "true" values of coefficients, *B(z)* and *D(z)*, in (2), we now solve the *direct problem*,

$$u_t^{dir} = D_n u_{zz}^{dir} + B_n u^{dir} + f(t) \tag{3}$$

for $(z,t) \in Q_T = [0,H] \times [0,T]$, with the IV and the BV's provided by the experimental solution, $u^{exp}$ (the data), i.e., imposing $u^{dir}(z, 0) = u^{exp}(z, 0)$, $u^{dir}(H, t) = u^{exp}(H, t)$, and $u^{dir}{}_z(0, t) = u^{exp}{}_z(0, t)$. The solution, so-evaluated numerically, is then *compared* with the solution (actually the change of the profile) obtained experimentally in $Q_T$ (the measured data, $u^{exp}(z, t)$). These two quantities, $u^{exp}(z, t)$ and $u^{dir}(z, t)$, favorably agree in $Q_T$ whenever the error, $\delta(z,t) = |u^{dir}(z,t) - u^{\exp}(z,t)|$ is "small", in some sense: point-wise, or in the maximum norm (that is its maximum value is small), or in the $L^2$ norm (that is in the square-mean, or rms) sense.

The inversion algorithm, which has been used in this paper, is similar to those, widely used to solve a number of the so-called *inverse problems*, see Lavrent'ev et al. (1986). It consists of

minimizing a certain "misfit functional" (or cost functional). Very often, the Fourier image of such a functional is minimized instead, which is an equivalent task, in view of Parseval identity. Here we use a version of this scheme, but we take, formally, the Laplace transform of the problem considered.

As for the numerical inversion, we, first recalculate the available data in terms of Laplace transforms, in order to obtain the data $U(z,\omega) = L[u(z,t)]$ and $F(\omega) = L[f(t)]$ . More precisely, in order to solve the problem, we use the Laplace-type representation

$$U(z,\omega) = \int_0^T u(z,t) e^{-\omega t} dt$$

with the formal inverse formula given by

$$u(z,t) = \frac{1}{T} \int_{\omega_1}^{\omega_2} U(z,\omega) e^{\omega t} d\omega$$

In this case, after formal Laplace transforming, the direct problem (3) for $U^{dir}(z,\omega)$ takes on the form

$$\frac{\partial^2 U^{dir}(z,\omega)}{\partial z^2} + \frac{B+\omega}{D} U^{dir}(z,\omega) = 0 \qquad (4)$$

with the boundary conditions given by

$$\frac{\partial U}{\partial z}\Big|_{z=0} = U_1(\omega) \qquad (5)$$

$$\frac{\partial U}{\partial z}\Big|_{z=H} = 0$$

$$U|_{z=0} = U_0(\omega) \qquad (6)$$

The cost functional we considered is

$$\Phi(B(z), D(z)) = \frac{1}{T} \sum_{n=-N}^{N} \int_0^H |U^{dir}(z,\omega_n) - U^{\exp}(z,\omega_n)|^2 dz \qquad (7)$$

for some *N*. Note that the appropriate domain of integration, and the data, $U^{dir}$, have been obtained solving a set of direct problems (each for every value of *n*).

The general idea here is to minimize the functional in Eq. 7 by choosing appropriate values of the coefficients *D(z)* and *B(z)*. The iterative procedure is as follows: we first guess certain values *D** and *B** of *D* and *B*, respectively, in Eq. 4, and then we solve numerically such equation with the boundary data given in Eq. 5, thus obtaining *U**. Then, we compute the current value of the functional in Eq. 7 corresponding to *U** for $U^{dir}$, and, based on some numerical method (the conjugate gradient method, e.g.), we make a new guess about the coefficients of the differential equation in such a way to attain a smaller value of the functional in Eq. 7.

STRUCTURE OF THR MEASURED DATA

The long-time evolution of the cross-shore position of coastal profiles was monitored during *39* years, from *1963* to *2001*, at Delfland, in The Netherlands (JARKUS dataset). This real data sets at each given point of the coast consists of a *100 x 39* array, corresponding to *100* observation points in space (i.e., in the *z* variable), each representing an average over *5* meters cross-shore, and *39* observation times, each representing an average over *1* year. The depth profiles have been studied only within a distance of *500* m from the coastline with a space step size of *5* m. Significant changes of the depth could be observed at the maximal distance where measures were made, at Delfland. Therefore, the space interval under consideration actually does not cover the distance of closure.

RECONSTRUCTING EQUATION COEFFICIENTS, TAKING INTO ACCOUNT CERTAIN AREA ALONG THE COAST

The functional given in Eq. 7 was used to recover the functions *D(z)* and *B(z)* in the governing Eq. 2, or, in fact, in the Eq. 4. Recall that in Avdeev et al (2009) similar problem were solved numerically using the experimental data obtained at the Ameland Island (in Holland), over 36 years, from 1963 to 1998. There, a special point at the coast was selected. Here we solve a similar problem, taking into account the full portion of the coast line located between the indicators 12.00 and 18.00 shown in the Fig. 1.

At the so-selected part of the coast 30 observation points were located at the distance of 200 m from each other. Measurements (depth versus distance from the given point at the coast) were taken once per a year. The number of points where the depth (cross shore) was measured varied from 70 to 150 opposite each point of the coast. Thus, an area of 3 km along the coast times about 1,5 km seaward was covered by measurements. The selected part of the coast is practically linear. Thus we did not expect dramatically large fluctuations in the values of model coefficients, *D(z)* and *B(z)*.

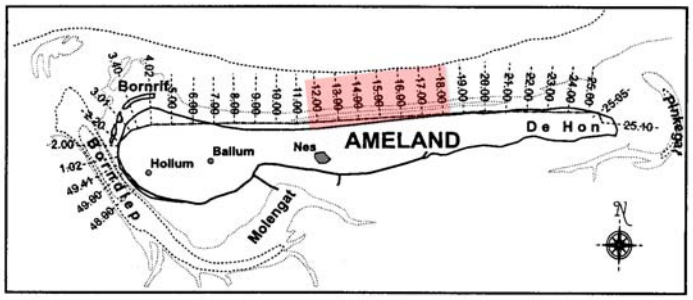

Fig. 1. Schematic map of the Ameland Island (above). The part of the coastline where the depth profiles have been used in the numerical experiments, is given in pink. A satellite image of Ameland Island is shown at the lower picture.

The measured data, used to minimize the cost functional in Eq. 7, is visualized in Fig. 2. The "horizontal" axis (going down from the left to the right) represents the years when the observations were made. The points along the coast are at the other axis, going up from left to right. Appreciable changes in depth (in meters) are observed on the vertical axis. The entire picture looks chaotic. A contour plot is given in Fig. 3, for convenience and future comparison. As it can be observed, the depth's deviation exceeds 3 meters in certain areas, and this phenomenon recurs from year to year.

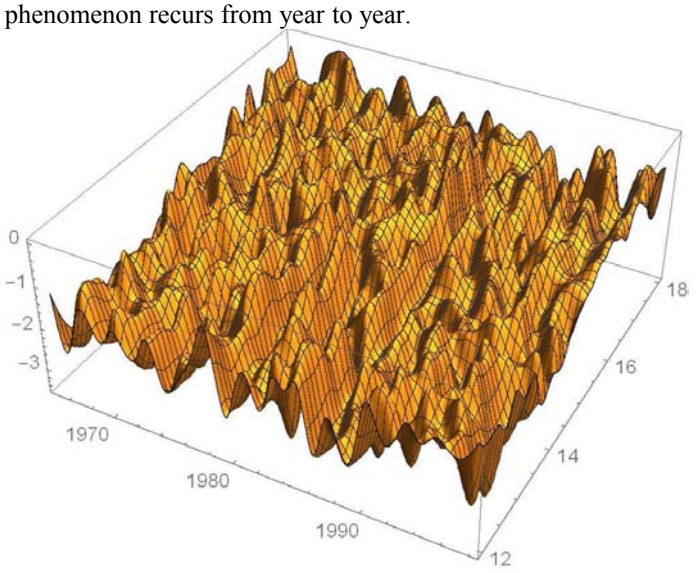


Fig. 2. Depth variations nearby the coast (virtually at z = 0), at all selected coastal observation points over the time when the observations were made. Vertical axis is calibrated in meters.

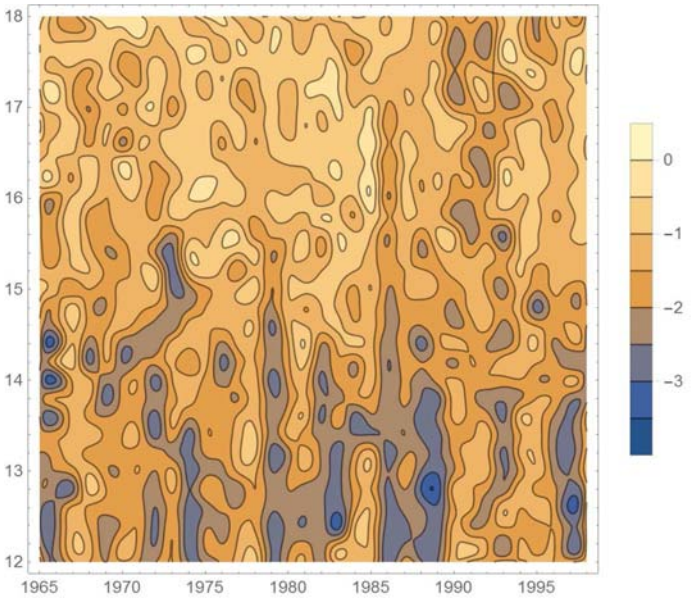


Fig. 3. Contour plot for the depth variation at the coast. The horizontal axis represents the years when the measurements were made, the vertical ones, observation points along the coast.

NUMERICAL RESULTS

In the first set of numerical tests, the coefficients, *D(z)* and *B(z),* were supposed constant at all 30 observation points along the coast. The following version of the misfit functional in Eq. 7 was considered in the form

$$\Phi(B(z),D(z))= \sum_{i=1}^{30}\int_{\omega}|U_0^i(\omega)-U_i^{dir}(0,\omega,D(z),B(z))|^2 d\omega \qquad (8)$$

The functions *D(z)* and *B(z)* were supposed to be constant at each interval 100 m, that is they take on 15 values each:

$$D(z) = d_n,\ B(z) = b_n,\ 100n < z < 100\,(n+1),\ n = 0,1,\ldots,14. \qquad (9)$$

The values of coefficients *D(z)* and *B(z)* in the form of Eq. 9, obtained numerically, are shown in Fig. 4.

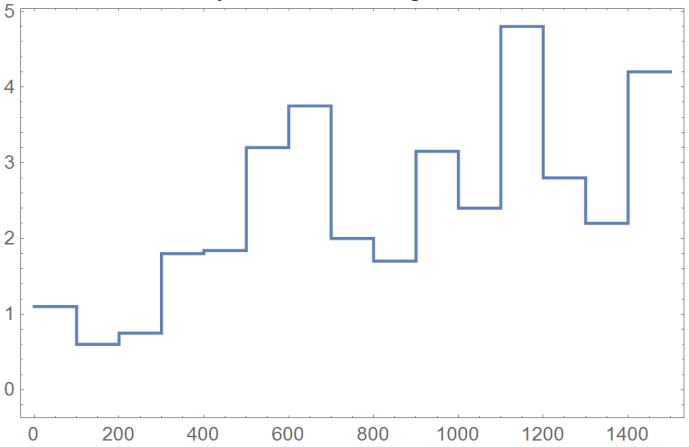

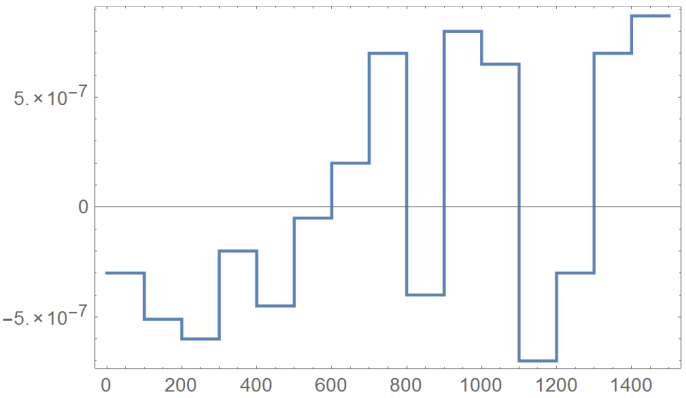


Fig. 4. Equation coefficients *D(z)* (above) and *B(z)* (below) for which the functional in Eq. 8 attains its minimum value. Both, *D(z)* and *B(z),* are piecewise constant functions as in Eq. 9.

As it was observed, the convergence of the numerical algorithm that implements the cost functional in Eq. 8 was faster compared to that of for the functional in Eq. 7 used for the single observation made along the coast. The value attained by the functional in Eq. 8 was

$$\Phi\left(B(z),D(z)\right)=41,5 \qquad (10)$$

The direct problem Eqs. 4~5 was solved, again, with the so-obtained piecewise constant coefficients in Eq. 9. We then compute the depth's variations close to the coast, as it was done previously using the measured data. The results are given in Figs. 5~6:

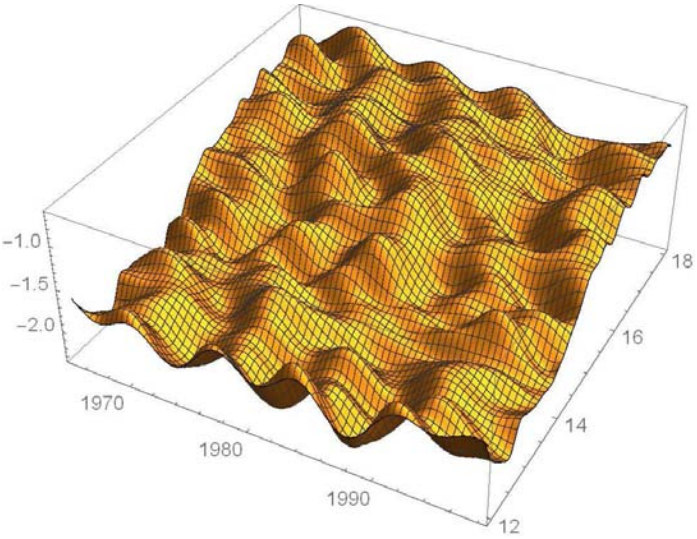


Fig. 5. Depth variations (cf. Fig. 2) close to the coast (virtually at $z = 0$), computed with the help of the coefficients *D(z)* and *B(z)* obtained numerically in the form of Eq. 9. The vertical axis is in meters.

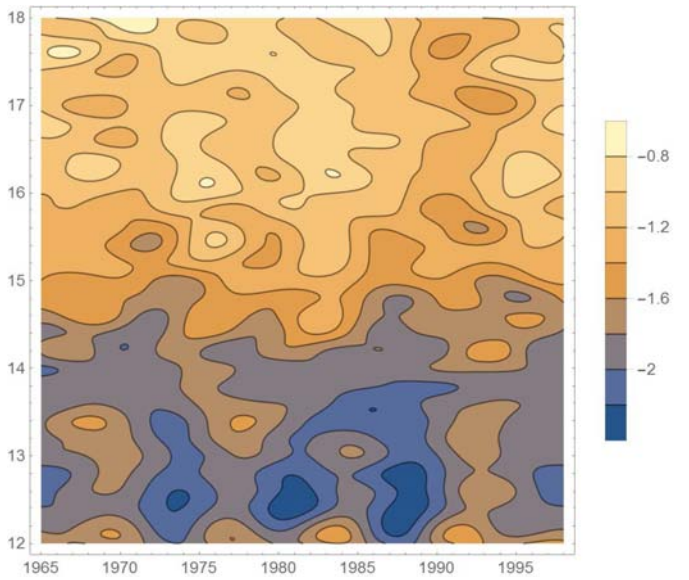


Fig. 6. Contour plot of the depth variation at the coast (cf. Fig. 3), computed by the help of the values of the coefficients *D(z)* and *B(z)* obtained numerically as in Eq. 9. The horizontal axis represents the years, the vertical one the observation points along the coast.

As it was observed, the qualitative behavior of the depth evolution agrees with what was observed, which fact is clear from Figs. 3 and 6.

In Figs. 7~8, the difference are shown between the measured data and the numerical solution to the direct problem for Eq. 4 with the obtained optimal values of coefficients in the form of Eq. 9. Even though the variation of such a difference looks similar to that in the original picture in Fig. 2, the average amplitude is essentially smaller that that and it does not exceed 1 m.

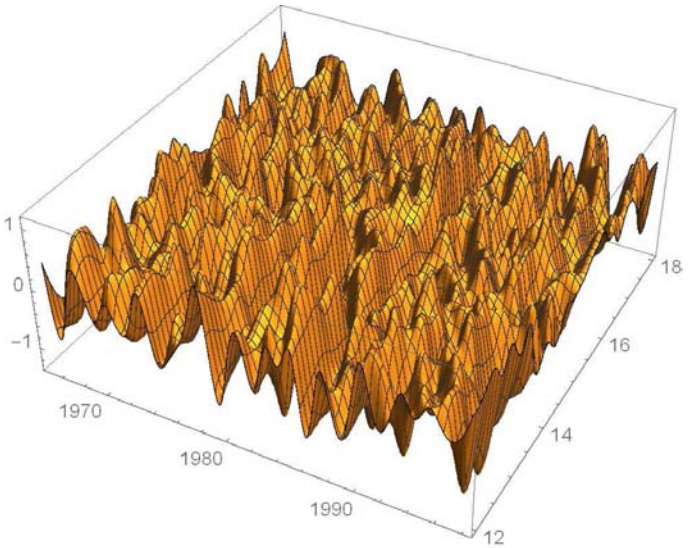


Fig. 7. Difference between the measured and the computed depth's variation nearby the coast, i.e., difference between the values shown on Figs. 2 and 5.

This phenomenon is clearer considering the contour plot of such a difference, depicted in Fig. 8. Definitely, the variations of the computed difference is distributed more uniformly compared to the original depth's variations of Figs. 3 and 6. Moreover, such a difference, in practice, does not exceed 1 m at any time and all locations.

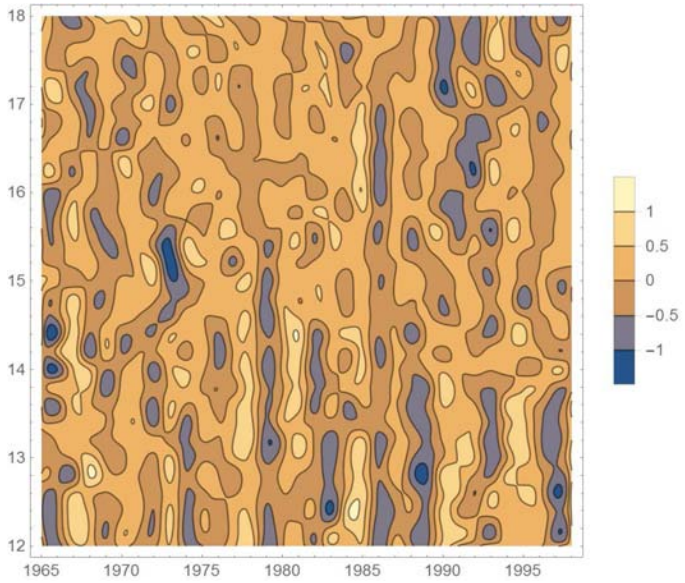


Fig. 8. Contour plot for the difference of values given in Fig. 7; compare to Figs. 3 and 6.

Finally, we admit variations of the coefficients, *D(z)* and *B(z)*, along the coast. Precisely, we suppose that both coefficients *D(z)* and *B(z)* takes three different values: $D_1(z)$ and $B_1(z)$ for the part of the coast line, located between the indicators 12.00 and 14.00 shown in the Fig. 1; $D_2(z)$ and $B_2(z)$ for the part between the indicators 14.00 and 16.00; and $D_3(z)$ and $B_3(z)$, for the part between the indicators 16.00 and 18.00. Each pair $D_i(z)$ and $B_i(z)$, i=1,2,3, has the form, given in Eq. 9.

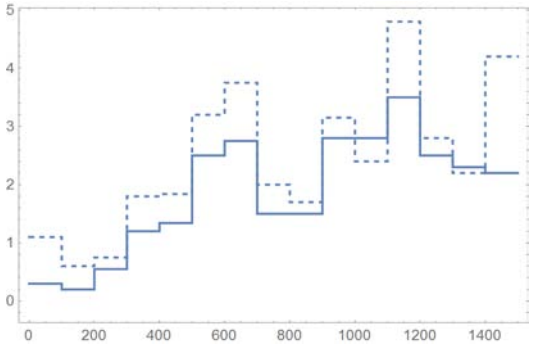


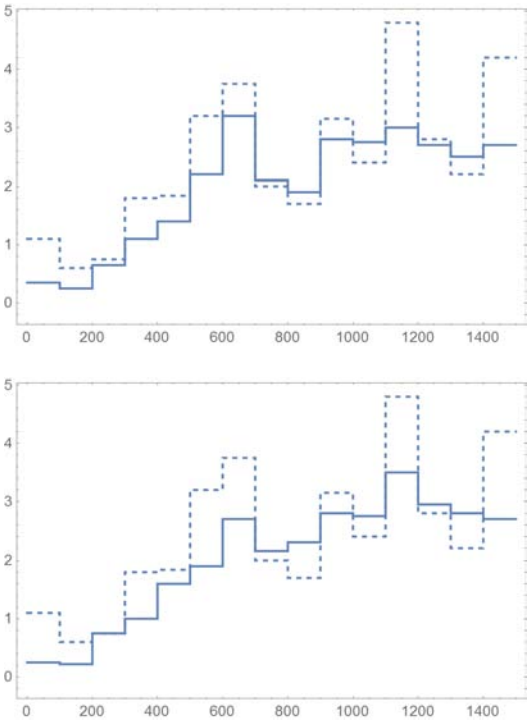


Fig. 9. The numerically obtained values of the coefficients $D_1(z)$ (above), $D_2(z)$ (middle), and $D_3(z)$ (below), in the form given in Eq. 9 are shown as solid line. The dashed line represents the values of *D(z),* obtained earlier and given in Fig. 4 (above).

The functional in Eq. 8 now takes the form

$$\Phi(B_1(z),D(z)_1,B_2(z),D_2(z),B_3(z),D_3(z))=$$
$$\sum_{i=1}^{10}\int_{\omega}|U_0^i(\omega)-U_i^{dir}(0,\omega,D_1,B_1)|^2\,d\omega+$$
$$\sum_{i=11}^{20}\int_{\omega}|U_0^i(\omega)-U_i^{dir}(0,\omega,D_2,B_2)|^2\,d\omega+ \qquad (11)$$
$$\sum_{i=21}^{30}|U_0^i(\omega)-U_i^{dir}(0,\omega,D_3,B_3)|^2\,d\omega$$

For initial guess we use the uniform (with respect to direction along the coast) optimal values of *D(z)* and *B(z),* in the form of Eq. 9, obtained earlier. These triples $D_i(z)$ and $B_i(z)$, *i = 1, 2, 3*, are shown in Figs. 9~10, respectively.

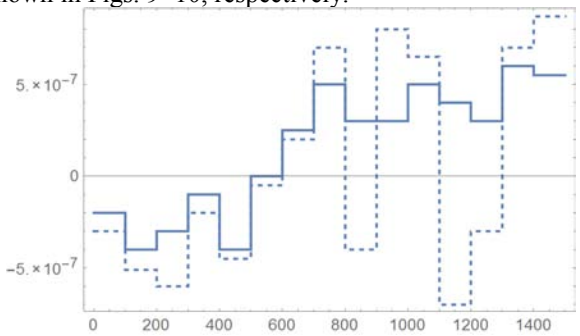

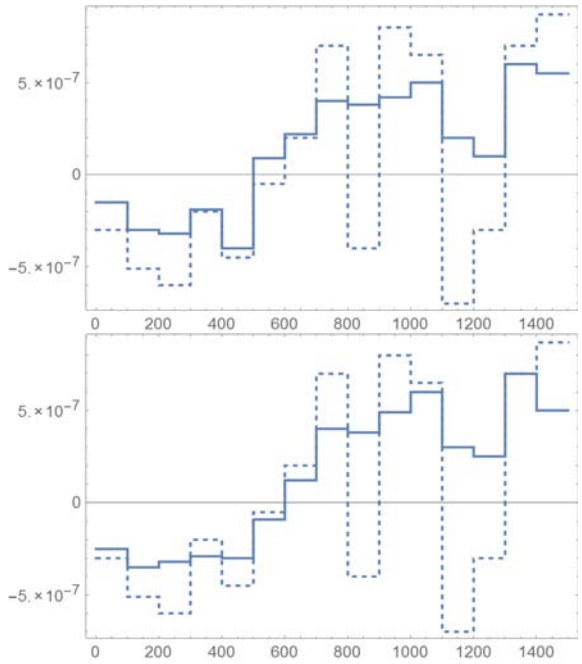


Fig. 10. The numerically obtained values of the coefficients $B_1(z)$ (above), $B_2(z)$ (middle), and $B_3(z)$ (below), given in the form of Eq. 9, are shown as solid line. The dashed line represents the values of $B(z)$, obtained earlier and given in Fig. 4 (below).

The value of the misfit functional in Eq. 11 turned out to be smaller, compared to the what found in the first numerical test, see Eq. 10:

$$\Phi(B_1(z), D_1(z), B_2(z), D_2(z), B_3(z), D_3(z)) = 32{,}3 \qquad (12)$$

As it can be observed in Figs. 9~10, the variations of the coefficients $D(z)$ and $B(z)$ become smaller. Figs. 11~12 show the simulated variations of depth at the coast using the triples $D_i(z)$ and $B_i(z)$, $i = 1, 2, 3$, and the corresponding contour plot (compare with Figs. 5~8).

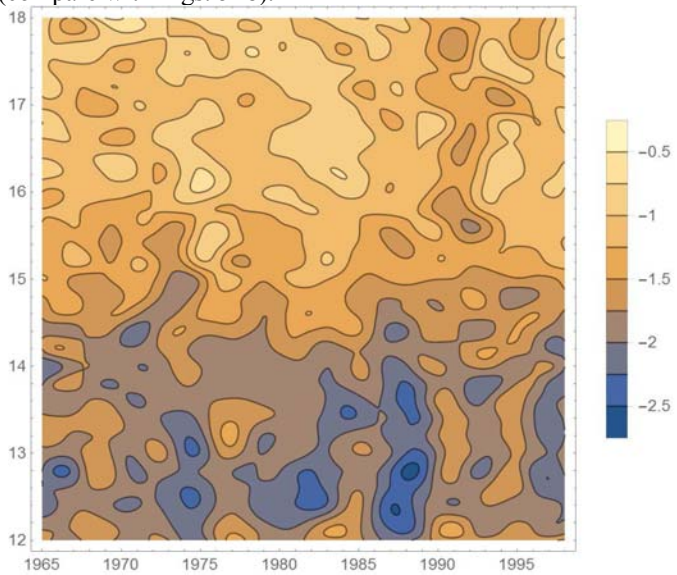


Fig. 11. Contour plot of the depth's variation at the coast, at $z=0$ (cf. Fig. 8), computed with the numerically obtained triples $D_i(z)$ and $B_i(z)$, $i = 1, 2, 3$.

Finally, as it was done in Figs. 7~8, we show the difference between the values of the measured data and those provided by the numerical solution to the direct problem in Eq. 4 with the optimal values of the triples for] the coefficients $D_i(z)$ and $B_i(z)$, $i = 1, 2, 3$ in the form of Eq. 9.

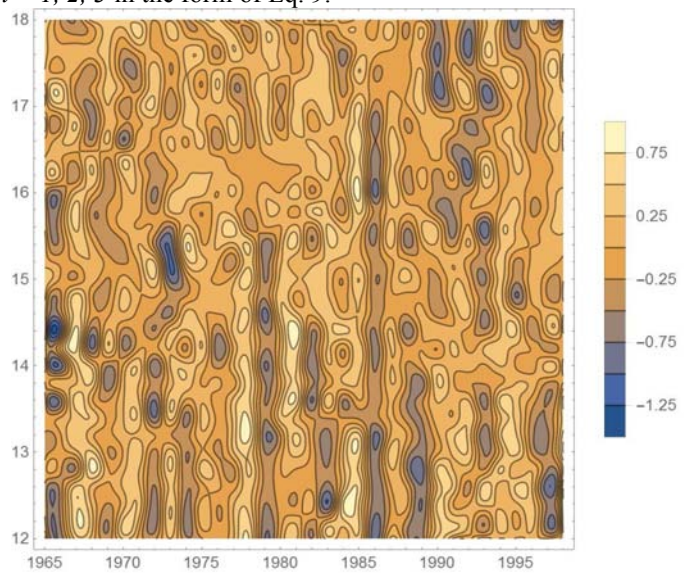


Fig. 12. Difference between the measured and the computed depth's variation close to the coast (**c**ontour plot, cf. to Fig. 8).

In Figs. 13~14 we also show the corresponding error for the computed values of the depth's profiles, according to the formula

$$\delta(0,t) = \left| \frac{u_{measured}(0,t) - u_{calculated}(0,t)}{u_{measured}(0,t)} \right| * 100 \qquad (13)$$

and the corresponding contour plot:

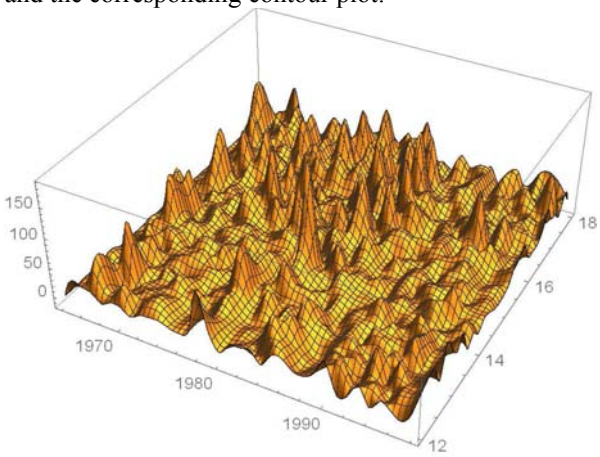


Fig. 13. Related error, computed according to Eq. 13, describing the coastal profile evolution with the help of the governing Eq. 4 and the optimal coefficients $D_i(z)$ and $B_i(z)$, $i=1, 2, 3$, given in Figs. 9~10.

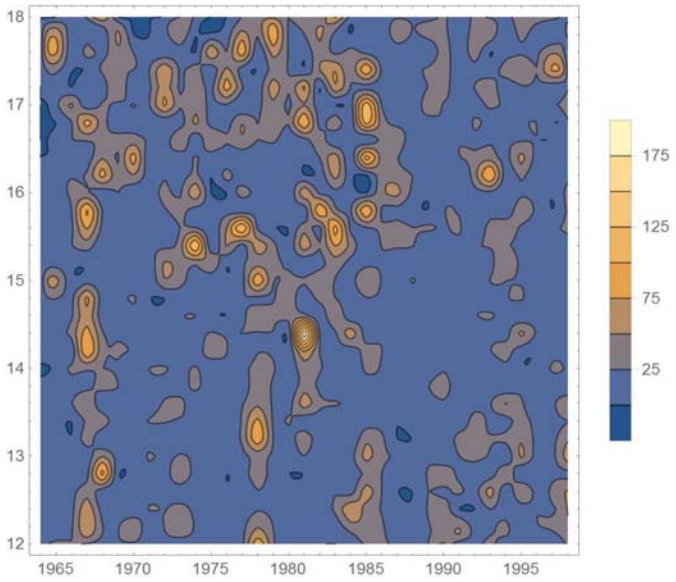

Fig. 14. Contour plot for the corresponding error, Eq. 13, given in Fig. 13.

## CONCLUSIONS

The diffusion model in Eq. 2 was used to describe the measured data of costal profile evolution. Upon an appropriate choice of the two coefficients, *B(z)* and *D(z),* modeled as piecewise constant functions, but depending on the distance from the shoreline, the depth profile evolution can be reasonable described on a rectangular region having the size of 3 km along the coast times about 1,5 km seaward. The model equation in Eq. 2 exploits data up to the so-called depth of closure, that is the distance from the shore where depth changes virtually end. Even though the available measured data does not possess this property, the numerical relative errors (see Eq. 13) are rather small over the entire area of observation.

## REFERENCES


Avdeev, AV, Goriounov, EV, Lavrentiev Jr., MM, and Spigler, R (2009). "A behavior-oriented model for long-term coastal profile evolution: Validation, identification, and prediction", *Applied Mathematical Modelling*, 33(10), 3981-3996.

Alekseev, AS, Avdeev, AV, Fatianov, AG, Cheverda, VA (1993). "Wave processes in vertically-inhomogeneous media: a new strategy for a velocity inversion", *Inverse Problems*, 9(3), 367-390 (IOP Publishing Ltd, UK)

Avdeev, AV, Lavrentiev Jr., MM, Goriounov, EV, and Spigler, R (1999). "Simultaneous identification of two coefficients in diffusion equation", *Bulletin of Novosibirsk Computing Center, series "Mathematical Modelling in Geophysics*", 5, 1-20.

Avdeev, AV, Lavrentiev Jr., MM, and Priimenko, VI (1999). *Inverse Problems and Some Applications*, Novosibirsk, ICM&MG, 342.

Bakker, WT (1968). "The dynamics of a coast with a groyne system", *Proc. 11th Coastal Engineering Conference*. - Amer. Soc. Civil Eng. (ASCE), 492-517.

Beavers, R, Howd, P, Birkemeier, W, and Hathaway, K (1999). "Evaluating profile data and depth of closure with sonar altimetry", *Proc. Hauppauge Coastal Sediments*, NY, 1, 479-490.

Capobianco, M (1992). "A procedure for parameter identification of partial differential equations of parabolic type", *G6-M Workshop ``System Dynamics''*, Delft Hydraulics.

De Vriend, HJ, Capobianco, M, Chesher, T, de Swart, HE, Latteux, B, and Stive, MJF (1993). "Approaches to long-term modelling of coastal morphology: a Review", *Coastal Engineering*, Elsevier Science Publ. B.V., Amsterdam, 21, 225-269.

Dean, RG (1991). "Equilibrium beach profiles: characteristics and applications", *J. Coastal Res*., 7(1), 53-84.

Hanson, H (1987). "GENESIS, a generalized shoreline change numerical model for engineering use", *Univ. of Lund, Dept. of Water Res. Eng.*, Report 1007.

Larson, M, Hanson, H, and Kraus, NC (1987). "Analytical solutions of the one-line model of shoreline change", *Report to U.S. Army Corps of Engineers, Coastal Engineering Research Center*, 6.

Lavrent'ev, MM, Romanov, VG, and Shishatskii, Y (1986). "Ill-Posed Problems of Mathematical Physics and Analysis", *AMS Translations of Math. Monographs* 64.

Vasiliev, FP (1981). "Methods of solving extremal problems", *Nauka, Moscow*.